SNOW-TOOLS

Research and development of remote sensing methods for snow hydrology

Relief effects for passive microwave remote sensing

WP 330

Christian Mätzler

Research Report No. 98-3
May 1998

See also: C. Mätzler and A. Standley, "Relief effects for passive microwave remote sensing", Internat. J. of Remote Sensing, Vol. 21, No. 12, pp. 2403-2412 (2000).

Dept. of Microwave Physics
Institute of Applied Physics
Sidlerstr. 5,
CH-3012 Bern
Switzerland

Tel. : +41 31 631 89 11
Fax. : +41 31 631 37 65
matzler@iap.unibe.ch

SNOW-TOOLS

Research and development of remote sensing methods for snow hydrology

Relief effects for passive microwave remote sensing

WP 330

Christian Mätzler, Daniel Hiltbrunner

[1]Institute of Applied Physics, University of Bern, Switzerland

Version 1.0, May, 1998

Contracts: BBW 95.0847, NENV4-CT96-0304
An Environment and Climate project
supported by the Swiss Bundesamt für Bildung und Wissenschaft and by the Commission of the European Community

1. Introduction

In order to assess potential error sources in current snow algorithms based on passive microwave data, the quantification of the different factors contributing to the result of the measurement of microwave radiation is necessary. This part deals with the effects of a terrain with variable height and with tilted surfaces on the measurement of microwave radiation by means of satellite-based radiometers.
The relief effects are twofold: First, the path between the radiation source at the surface and the sensor depends on the surface height, thus leading to a height-dependent atmospheric contribution. This main relief effect is the topic of Section 2, where the radiation from a horizontal surface with a flat horizon at a given altitude is assumed. Section 3 is devoted to a variable topography consisting of valleys and ridges; the characteristic effects on the passive microwave signal will be described.

2 Flat horizon

The classical model geometry of remote sensing of the terrestrial surface is a pair of half spaces separated by a horizontal surface, leading to a flat horizon at all scales. In this situation there is no shadow of any kind. The relief effects are determined by the dependence of the emitted radiation on the altitude *h* of the surface. Blackbody radiation with a brightness temperature equal to the physical temperature T_0 is produced in the lower half space, part of which is transmitted, and thus emitted (T_e) into the upper half space where it is sensed by a radiometer (Figure 1). Radiation from the upper to the lower half space (T_{sky}) is much smaller than T_0.

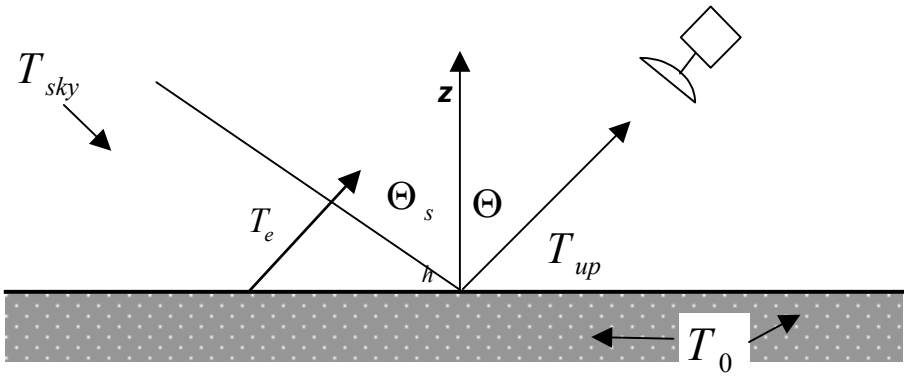

Figure 1: Emitted brightness temperature T_e above a horizontal surface of emissivity e_p =1-r_p (p = polarization *h* or *v*) at physical temperature T_0 illuminated from sky by T_{sky}.

The *p*-polarized emitted brightness temperature T_e above a flat surface with reflectivity r_p is given by

$$T_e = e_p T_0 = (1-r_p)\, T_0 \qquad (1)$$

(The direction ***k*** into which the radiation is emitted is just opposite to the direction of the incident radiation for which r_p is the reflectivity.) The upwelling radiation just above the surface is the sum of the radiation emitted by the lower space and the radiation T_{sky} incident from the upper half space and being reflected at the surface towards the sensor:

$$T_{up} = (1-r_p)T_0 + r_p\, T_{sky} \qquad (2)$$

The brightness temperature T_b at satellite level is the attenuated upwelling radiation plus the radiation emitted by the atmosphere in the direction toward the radiometer (atmospheric scattering and atmospheric temperature inhomogeneity being neglected):

$$T_b(\theta) = T_{up}\, t + T_a\,(1\text{-}t) \tag{3}$$

where t is the atmospheric transmissivity in the observation direction and T_a is the temperature of the atmosphere. The above equation applies to the polarization and direction corresponding to T_{up}. In case of an inhomogeneous atmosphere T_a has to be considered as an effective temperature $T_{a,up}$ for upwelling radiation. The transmissivity is given by

$$t = \exp(-\tau_h/\cos\theta) \tag{4}$$

where

$$\tau_h = \int_h^\infty \alpha(z)dz \tag{5}$$

is the zenith opacity of the atmosphere at the surface, and $\alpha(z)$ is the absorption coefficient of the atmosphere at altitude z. The reflectivity r_p at polarization p = h, v in (2) may be composed of a specular component $r_{s,p}$ at polarization p and of a diffuse, unpolarized component r_d :

$$r_p = r_{s,p} + r_d \tag{6}$$

The following discussion is concentrated on the derivation of expressions for T_{up} depending on properties of the relief. We will assume that we can approximate the total reflectivity r_p by (6), where $r_{s,p}$ is a perfectly specular component and r_d is a lambertian component, i.e. due to a perfectly rough surface. In Ulaby et al. (1981, Sec. 4-16.2), $r_{s,p}(\Theta)$ and r_d are expressed by $\Gamma(\Theta_0, p)$ and $0.25\sigma_0^0$, respectively, where Θ is the observation angle with respect to the surface normal, and p is the state of polarization (p = v, h).
According to Ulaby et al. (1981), T_{up} can be written as

$$T_{up}(\Theta, h) = e_p(\Theta)T_0 + r_{s,p}(\Theta, p)T_{sky}(\Theta, h) + \frac{\sigma_0^0}{4\pi}\iint T_{sky}(\Theta_s, \Phi_s, h)\cos\Theta_s d\Omega_s\ , \tag{7}$$

where h is the height of the surface above sea level. The integral term in (7) is the diffusely scattered sky radiation, here to be called T_d ; as a result of Lambert scattering T_d depends only on h. We assume that the incident sky radiation is unpolarized. For a plane-parallel atmosphere T_{sky} depends on Θ_s and h, thus the integral in (7) can be solved for Φ_s using $d\Omega_s = \sin\Theta_s d\Theta_s d\Phi_s$:

$$T_d(h) = \frac{\sigma_0^0}{2}\int_0^{\pi/2} T_{sky}(\Theta_s, h)\cos\Theta_s \sin\Theta_s d\Theta_s\ . \tag{8}$$

In case of an isothermal atmosphere at temperature T_a with a cosmic background T_c we have

$$T_{sky}(\Theta_s, h) = T_c e^{-\tau_h/\cos\Theta_s} + (1 - e^{-\tau_h/\cos\Theta_s})T_a\ , \tag{9}$$

Equation (9) can be used even for a non-isothermal atmosphere; then T_a is an effective air temperature $T_{a,down}$ for downwelling radiation (Mätzler, 1992; Ingold et al., 1998). We obtain

$$T_d - T_c = \frac{\sigma_0^0}{2}(T_a - T_c)\int_0^{\pi/2}(1 - e^{-\tau_h/\cos\Theta_s})\cos\Theta_s \sin\Theta_s d\Theta_s, \tag{10}$$

where σ_0^0 is a constant related to the dielectric properties of the scattering surface. For an optical thin atmosphere ($\tau_h << 1$) the exponential in (10) can be replaced by the first two terms of the Taylor series expansion

$$e^{-\tau/\cos\Theta} \cong 1 - \tau_h/\cos\Theta_s, \tag{11}$$

which leads to

$$T_d - T_c = \frac{\sigma_0^0}{2}(T_a - T_c)\tau_h \int_0^{\pi/2}\sin\Theta_s d\Theta_s = r_d \cdot 2\tau_h(T_a - T_c), \tag{12a}$$

where σ_0^0 has been replaced by $4r_d$. As pointed out by Mätzler (1987), the brightness temperature T_d can be observed from the surface looking up at the incidence angle $\Theta = 60°$, i.e. for 2 air masses ($\cos\Theta$ = ½). The exact integration of (10) leads to

$$T_d - T_c = r_d(T_a - T_c)\left[1 - 2E_3(\tau_h)\right], \tag{12b}$$

where E_3 is the exponential integral of order n=3. The integral is defined by $E_3(\tau_h) \doteq \int_1^\infty \frac{e^{-\tau_h y}}{y^3} dy$ (Abramowitz & Stegun, 1974). Eventually, we get

$$T_{up} = T_0 e_p(\Theta) + T_a r_p - (T_a - T_c)\left[r_{sp}\exp(-\tau_h/\cos\Theta) + r_d 2E_3(\tau_h)\right], \tag{13a}$$

with $e_p + r_p = 1$ and $r_p = r_{sp} + r_d$. Another representation of T_{up} is obtained if we write $2E_3(\tau_h)$ as an effective transmissivity $t_d = 2E_3(\tau_h) = \exp(-\tau_h/\cos\Theta_d)$, by taking Θ_d as an effective incidence angle for diffuse radiation. For an optically thin atmosphere ($\tau_h \to 0$) we get $\Theta_d = 60°$ and $\cos\Theta_d$ = ½ (see discussion in Mätzler 1987). Following this representation, we get

$$T_{up} = T_0 e_p(\Theta) + T_a r_p(\Theta) - (T_a - T_c)\left[r_{sp}(\Theta)t(\Theta) + r_d t_d\right], \tag{13b}$$

where the atmospheric transmissivity is defined as

$$t(\Theta) = \exp(-\tau_h/\cos\Theta) \tag{14}$$

A simplification occurs if $\Theta = \Theta_d$; then $t = t_d$ and

$$T_{up} = T_0 e_p(\Theta_d) + T_a r_p(\Theta_d) - (T_a - T_c) r_p(\Theta_d) t_d \quad (15)$$

Now, since Θ_d is often between 50° and 60° and since this is also the case for the nadir angle Θ of conical scanning sensors on satellites (SMMR, SSM/I, AMSR), this simplified formula has been used frequently. It is to be noted that the difference between (13) and (15) is negligible if at least one of the following conditions is valid:

- the atmosphere is sufficiently transparent ($t_d \cong 1$),
- $\theta \cong \theta_d$,
- $r_d \cong 0$.

After having found the most applicable expression for T_{up} we can determine its value from surface and atmospheric properties. Inserting T_{up} in Equation (3) leads to the relief-dependent radiation at satellite level, i.e. the dependence of T_b on h. Note that both T_{up} and t depend on h. It is to be expected that this altitude dependence is the dominant relief effect, especially if the frequency is above 20 GHz, and if the height variation is significant.

3 Terrain with tilted surfaces

In addition to the altitude effects on atmospheric radiation described above, there are relief effects due to tilted surfaces. On the one hand the local incidence angle on a tilted surface depends on the orientation of the surface with respect to the view direction of the sensor, and on the other hand the tilted surfaces lead to a variable and elevated horizon depending on azimuth, shadowing parts of the open sky. In these directions the incident sky radiation is replaced by the emission of the elevated landscape.

Because the scale of the relief is assumed to be large with respect to the sensing wavelength, both effects (at the large scale) can be described by scattering models using geometrical optics. A facet model is indicated, see e.g. Schanda (1986, Section 4.3); such a model was used to describe the microwave emission of the rough sea surface at mm wavelengths by Prigent and Abba (1990) who assumed each facet to be a specularly reflecting surface element. In contrast to their model we must allow, in accordance to Section 2, that the surface elements have a partly-specular and a partly-lambertian component.

3.1 Emission from large-scale rough surfaces

Reflection on and emission from a local surface facet can be treated as in Section 2 with the exception that the surface normal **n** used to define the plane of incidence deviates from the vertical direction **z** by a tilt angle α, oriented by an azimuth angle ϕ with respect to the global plane of incidence (Figure 2). The transformation from the global to the local plane of incidence affects both the scattering geometry and the polarization. The local angle of incidence θ_l is given by

$$\cos\theta_l = \sin\theta \sin\alpha \cos\phi + \cos\theta \cos\alpha \quad (16)$$

Furthermore the linear polarization is rotated by an angle φ given by

$$\sin\varphi = \sin\phi \sin\alpha / \sin\theta_l \quad (17)$$

After the reflectivities $r_{vl}(\theta_l)$ and $r_{hl}(\theta_l)$ have been determined in the local reference frame they can be represented in the global (satellite-earth surface) frame taking into account the polarization rotation:

$$r_v(\theta) = r_{vl}(\theta_l) \cos^2\varphi + r_{hl}(\theta_l) \sin^2\varphi \quad (18)$$
$$r_h(\theta) = r_{vl}(\theta_l) \sin^2\varphi + r_{hl}(\theta_l) \cos^2\varphi \quad (19)$$

In our choice of the reflectivity this transformation only acts on the specular components $r_{s,p}$, since r_d is independent of incidence angle and polarization.

3.2 Shadowing effects

When we speak about shadows we have some active, directed illumination in mind for a given incidence ray. Therefore it may not be quite clear what we mean in the present case of passive microwave radiation. First, the concept can be generalized to diffuse radiation just by adding the contributions to the radiance in the observation direction scattered from all incident rays. The incidence radiation is distributed over the half space above the local facet. Second the concept can be applied to passive radiation by Kirchhoff's law where emission is just the complement to scattering. By doing so we find the following effects:

- Shadowing effects include the influence of surface-scattered radiation emitted by some other part of the surface due to the fact that the sky is hidden by the elevated horizon. This means that the incident radiation is composed of a sky term and of a terrestrial term.
- Certain facets appear enhanced or reduced in size (i.e. view solid angle), or are even hidden from a given view direction.

Both effects are to be described here, starting with the latter, see Figure 2. For a visible facet, the contribution to the received radiation depends on the solid angle Ω under which the facet appears; it is given by the relationship $\mathrm{A}\cdot\cos\Theta_1/\mathrm{R}^2$, where A is the true surface area of the facet and R is the distance to the radiometer antenna. Now, a surface area is usually represented on a map by its projection A_h on a horizontal plane. If we use this projected area, then we get for Ω

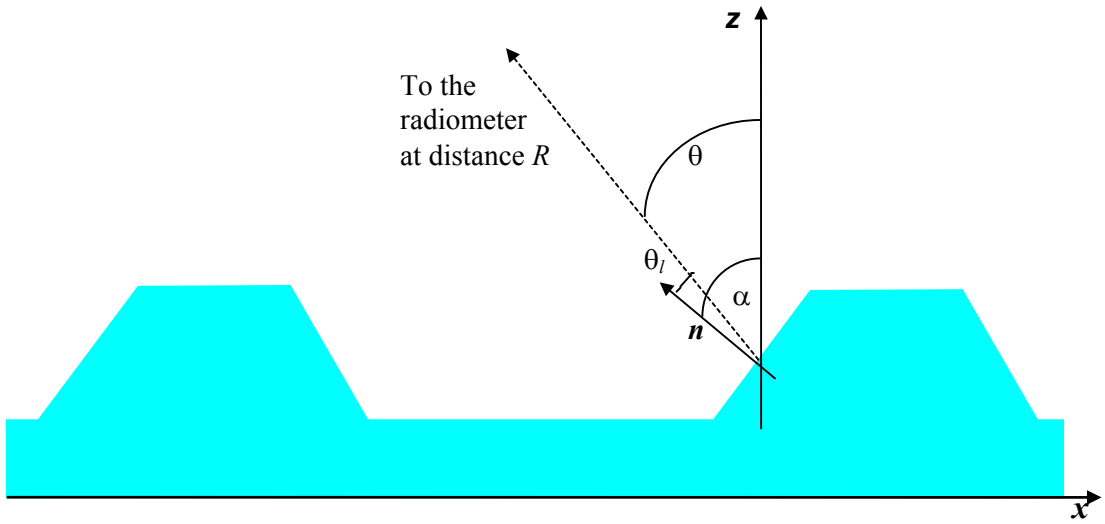

Figure 2: Local θ_l and global θ incidence angles on a surface tilted by angle α.

$$\Omega = \frac{A_h \cos\Theta_l}{R^2 \cos\alpha} \tag{20}$$

where θ_l is again the local incidence angle of the facet. Now, the total signal at a given polarization collected by the radiometer antenna is a beam-weighted sum over the radiation from all facets (numbered from j=1 to n) within the antenna footprint:

$$T_{b,total} = \frac{1}{\Omega_{total}} \sum_{j=1}^{n} T_b(A_j)\cdot\Omega_j \tag{21}$$

The above summation is limited to the nearest facet per line of sight, taking the closest one to the radiometer.

The remainder of this section will be devoted to the estimation of the former effect, assuming that the surface is a Lambert scatterer ($r_v = r_h = r_d$). Let us consider a horizontal profile in some direction ***x*** through a landscape as shown in Figure 3. The profile elements are straight lines whose ends have x coordinates x_1, x_2, x_3, etc. For illustration purposes the landscape is simplified to table mountains in a horizontal plain.

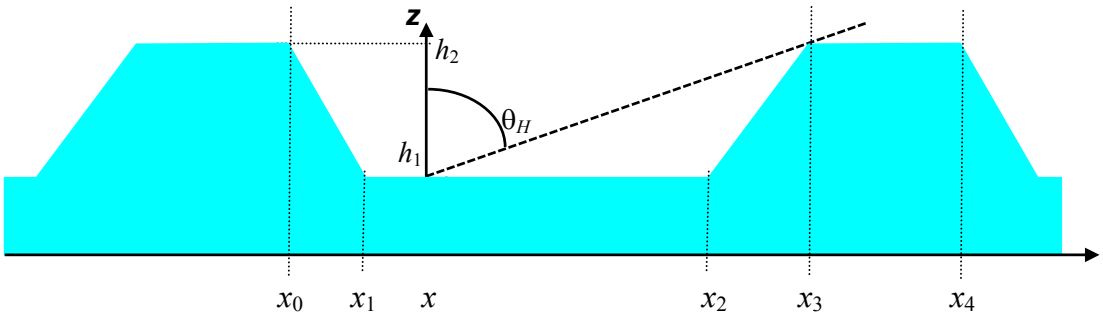

Figure 3: Profile through a simple landscape to illustrate the horizon at position x.

The quantity of interest is the zenith angle θ_H of the horizon to the right in Figure 3 at position x ($x_0 \le x \le x_4$). The slope tangent b of the dashed line, i.e. $b(x) = \cot\theta_H$ is given by

$$b(x) = \begin{cases} \dfrac{(h_2 - h_1)}{(x_1 - x_0)} \dfrac{(x - x_0)}{(x_3 - x)}; & x_0 \le x \le x_1 \\ \dfrac{h_2 - h_1}{x_3 - x}; & x_1 \le x \le x_2 \\ \dfrac{h_2 - h_1}{x_3 - x_2}; & x_2 \le x \le x_3 \\ 0 \quad ; & x_3 \le x \le x_4 \end{cases} \tag{22}$$

The sky radiation is limited to incidence angles θ smaller than θ_H. For larger angles enhanced incident radiation appears from the elevated landscape. The brightness temperature of this radiation is denoted by T_h. Let us define the total upwelling brightness temperature by T_{up} (total) as the sum of the radiation from a flat horizon, T_{up} (Section 2), plus the increase ΔT_{up}, i.e.

$$T_{up}(\text{total}) = T_{up}(\text{Section 2}) + \Delta T_{up}. \tag{23}$$

The increase can be written as

$$\Delta T_{up} = \frac{r_d}{\pi} \int_0^{2\pi} d\beta \left(\int_{\theta_H}^{\theta_{\max}} T_h(x,\theta) \cos\theta \sin\theta \, d\theta - \int_{\theta_H}^{\pi/2} T_{sky}(\theta) \cos\theta \sin\theta \, d\theta \right) \tag{24}$$

The angle β is the azimuth angle of the surface-profile direction. The upper limit in the first θ integral is denoted by θ_{max}. This value is π/2 for a horizontal facet, but for a tilted facet, θ_{max} may be larger or smaller depending on the orientation of the facet (i.e. the integration has to include all incident directions of the local facet). Note that values of θ_H and θ_{max} depend on azimuth β.

Let us add a short comment for the case of a partly specular facet: The above expression for ΔT_{up} is still valid as long the specularly reflected component emanates from the sky. This situation can easily be checked at least for horizontal facets. In other situations where specularly reflected radiation emanates from the surface elements, a ray-tracing technique has to be applied to include all multiple reflections and emissions. In a statistical sense the overall appearance of a very rough surface is one that behaves more and more like a lambertian one.

Now we return to Equation (24) to estimate the increase ΔT_{up} for a lambertian facet. In the simplified case of a horizontal facet at the lower altitude h_1 where $\theta_{max}=\pi/2$ we have

$$\Delta T_{up} = \frac{r_d}{\pi} \int_0^{2\pi} d\beta \int_{\theta_H}^{\pi/2} \left[T_h(x,\theta) - T_{sky}(\theta) \right] \cos\theta \sin\theta \, d\theta \tag{25}$$

In order to estimate an upper limit $\Delta T_{up,max}$ of ΔT_{up}, we assume that the elevated surface is a black body (T_h=T_0) and that the zenith opacity is negligible (T_{sky} = T_c). This situation is approximated by a forest-covered hill at a frequency below about 15 GHz. These simplifications lead to

$$\Delta T_{up,max} = \frac{r_d (T_0 - T_c)}{\pi} \int_0^{2\pi} d\beta \int_{\theta_H}^{\pi/2} \cos\theta \sin\theta \, d\theta = \frac{r_d (T_0 - T_c)}{2\pi} \int_0^{2\pi} d\beta \cos^2 \theta_H$$
$$= r_d (T_0 - T_c) \overline{\cos^2 \theta_H} \qquad (26)$$

where the horizontal bar in the last expression means averaging over azimuth direction. With this expression it is rather simple and straightforward to compute $\Delta T_{up,max}$ using a Digital Elevation Model (DEM). The key quantity is the square of $\cos\theta_H$.; it can be computed from *b(x)*:

$$\cos^2 \theta_H = \frac{1}{1 + b^{-2}} \qquad (27)$$

Let us assume a typical hilly relief with an average θ_H of 80° and with an average $\cos^2\theta_H$ of 0.17^2 ≅0.03. In order to produce a noticeable increase ΔT_{up}, the diffuse reflectivity r_d has to be large enough. For r_d < 0.2 the correction is negligible. The effect gets stronger as the ruggedness of the terrain increases. In an area dominated by steep slopes the mean value of $\cos^2\theta_H$ within deep valleys may reach something like 0.5. Since such regions have limited lateral extent, their overall contribution to the radiometer pixel value may still not be very important. In a further situation we assume that besides a constant surface temperature T_0, the surface reflectivity r_p is everywhere the same and given by r_d. Then, if the zenith opacity is still negligible, ΔT_{up} becomes

$$\Delta T_{up} \cong \; r_d (1 - r_d) \left[T_0 - T_{sky} \right] \overline{\cos^2 \theta_H} \qquad (28)$$

The only difference with respect to (26) is the additional factor (1-r_d). If the reflecting facet is a tilted surface we can still use the above expressions for ΔT_{up}, however, with θ_H being the local angle of incidence of the horizon. At low elevation angles, however, the atmospheric emission is often not negligible. Increasing atmospheric contribution reduces ΔT_{up} to values closer and closer to zero, and may thus become negligible. Numerical simulations of ΔT_{up} using DEM and realistic atmospheric data should be applied to quantify the actual behavior. The simulations could be used to correct this special relief effect for given regions and seasons.

4 Conclusions

We considered relief effects on the upwelling brightness temperature T_{up} at the surface and on the brightness temperature T_b to be observed by a satellite. The formulas were derived for surfaces whose reflectivity can be described by a partly specular and a partly lambertian scattering behavior. Apart from horizontal surfaces with a flat horizon the shadowing effects of a hilly terrain with an elevated horizon were included, especially for lambertian surfaces. These effects can be expressed by an increase ΔT_{up} of T_{up}. The formulas for ΔT_{up} are also valid if a specular component exists as long as the specularly reflected rays do not lead to an additional increase of T_{up}. A ray-tracing method would be required to model multiple specular reflections. In addition to shadowing effects tilted surfaces lead to changes in incidence angle and to a rotation of the plane of linear polarization.
It appears that the main relief effects result from the variable atmospheric contributions due to their dependence on the altitude *h* of the emitting surface. Together with realistic atmospheric data the formulas should be applied to rugged regions to quantify the actual behavior. Finally, it should be emphasized that the exact computation of the shadowing effects is only possible if the bistatic scattering coefficient of the surface is known. The results of Section 3 are linked to the classical choice where the diffuse surface scattering can be represented by the Lambert cosine law.

References

Abramowitz M., Stegun I., 1974: Handbook of Mathematical Functions, New York: Dover.

Ingold T., Peter R., Kämpfer N., 1998: Weighted Mean Tropospheric Temperature and Transmittance Determination at mm-Wave Frequencies for Ground-Based Applications. Radio Science, Vol. 33, pp. 905-818.

Mätzler C., 1987: Applications of the Interaction of Microwaves with the Seasonal Snow Cover. Remote Sensing Reviews, Vol. 2, pp. 259-387.

Mätzler C., 1992: Ground-based measurements of atmospheric radiation at 5, 10, 21, 35 and 94 GHz. Radio Science 27, pp. 403-415.

Prigent, C. and P. Abba, 1990: Sea-surface equivalent brightness temperature at millimeter wavelengths, Annales Geophysicae, Vol. 8, pp. 627-634.

Schanda E. 1985: Physical Fundamentals of Remote Sensing, Springer-Verlag, Berlin.

Ulaby F.T., Moore R.K., Fung A.K., 1981: Microwave Remote Sensing, Active and Passive. Vol. I., Addison-Wesley Publ., Reading, Massachusetts.